

# The study of the Asymmetrical Half-Bridge Converter With magnetic coupled post regulator

Byeong-cheol Hyeon, Bo-Hyung Cho

School of Electrical Engineering and Computer Science  
Seoul National Univ. #043, San65-1, Sillim-dong, Gwanak-gu, Seoul, 151-744

## Abstract

In this paper, a multiple-output converter using a coupled-inductor is proposed. The Asymmetrical Half-Bridge Converter (AHBC), which is used as a master converter, obtains ZVS in the primary side switches. For the tight output voltage regulation of the slave output, the Secondary Side Post Regulator (SSPR) is adopted. The proposed magnetically coupled output filter inductor reduces the number of semi-conductor devices and magnetic components. Also, the circuit enables ZCS off switching in the SSPR MOSFET and rectifying diodes. The modes of operation which are caused by the coupled-inductor and post regulator are explained. The analyzed modes of operation of the proposed multiple-output converter are verified by the simulation and experimental results.

## 1. Introduction

As the analog and digital electronics become more complicated and advanced, they require several voltage sources in one electronics system. For the industrial demand, a number of DC/DC converters are required in the system and these converters increase the overall system cost, size and complexity. To deal with these challenges, various multiple-output approaches have been proposed [1]-[3]. As the system requirement for each output regulation specification becomes tighter, the cross-regulation may not be feasible, especially for a wide varying load conditions. Therefore a post regulator scheme should be used in a multiple-output converter to overcome the limitations of the cross-regulation [4] [5].

In this paper, a post regulator scheme using a coupled-inductor, as shown in Fig.1, is proposed. It reduces the number of magnetic cores through the integration of the output inductor. The freewheeling diode in the conventional circuit is removed because the inductor (or switch) current became zero before  $S_3$  turns off. By properly controlling the switch timing, the SSPR switch can achieve ZCS turn on and ZCS turn off through the fast current commutation in the transformer,  $T_2$ , without effective duty loss. As a master power stage, the AHBC is used for its inherent soft switching in the MOSET and the clamped switch voltage as were described in [6]-[7].

## 2. Analysis of the proposed converter

### 2.1 The modes of operation

The operation of the proposed converter, shown in Fig.2, is analyzed. For the slave output regulation, a buck type with tailing edge modulation is used. To simplify the steady state analysis several assumptions are made; (a) Switches  $S_1$ ,  $S_2$ ,  $S_3$  are ideal except for the parasitic capacitances  $C_1$ ,  $C_2$  and body diodes  $D_{S1}$  and  $D_{S2}$ . (b)  $V_{O1}$  and  $V_{O2}$  are constant during the switching period.

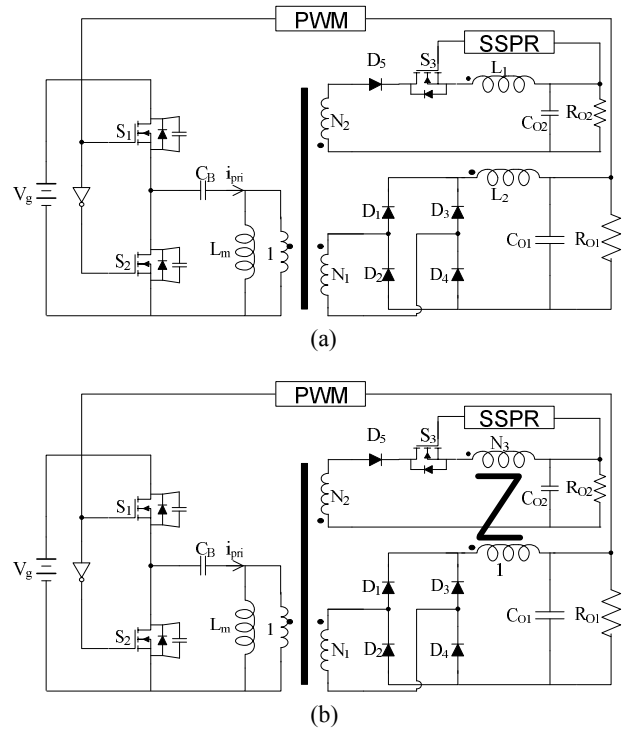


Fig. 1 The circuit configuration of the multiple-output converter (a) Conventional circuit. (b) Proposed circuit.

(c) The ideal transformers with leakage and magnetizing inductances are modeled for  $T_1$  and  $T_2$ . The sub-fix of the voltage and current follows the corresponding component names.

### Mode1 [ $t_0 \sim t_1$ ]

During Mode1,  $S_1$  is on and  $S_2$ ,  $S_3$  are off.  $i_1$  flows through  $D_1$ ,  $D_4$  and  $L_{m2}$ , which is magnetizing inductance of  $T_2$ . During this mode, the slave part is blocked by  $D_5$  and thus no energy is transferred. The currents are expressed in (1)-(2).

$$i_1(t) = \frac{(N_1(1-D)V_g - V_{O1})}{L_{m2}} t, \quad i_{m1}(t) = \frac{(1-D)V_g}{L_{m1}} t, \quad (1)$$

$$V_{m2}(t) = (N_1(1-D)V_g - V_{O1}) \quad (2)$$

### Mode2 [ $t_1 \sim t_2$ ]

During Mode2, the  $S_2$  voltage becomes zero and the primary side current of the transformer changes its direction

### Mode3 [ $t_2 \sim t_3$ ]

Mode3 starts when  $S_2$  is turned on. The current  $i_1$  flows through  $D_2$ ,  $D_3$  and  $L_{m2}$ . The slave part is blocked by  $S_3$ . The current

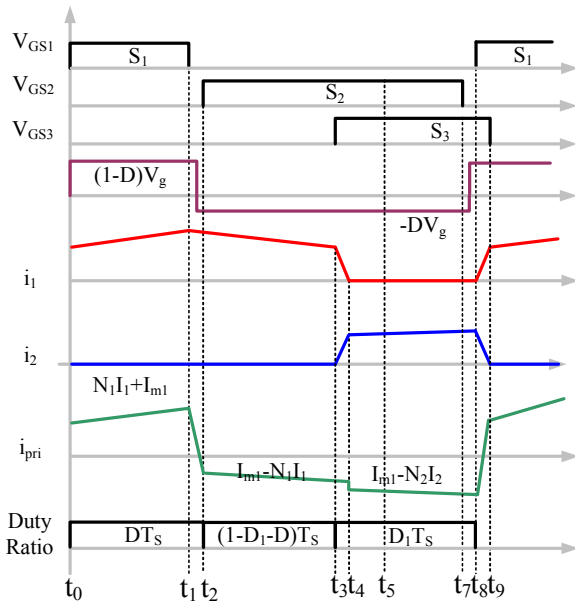


Fig. 2 The operating waveforms equations are shown in (3).

$$i_1(t) = \frac{N_1 DV_g - V_{O1}}{L_{m2}} t, \quad i_{m1}(t) = \frac{-DV_g}{L_{m1}} t \quad (3)$$

#### Mode4 [t<sub>3</sub>~t<sub>4</sub>]

Mode4 begins when S<sub>3</sub> is turned on. The current i<sub>2</sub> starts to increase and current i<sub>1</sub> decreases. In this mode, i<sub>1</sub> and i<sub>2</sub> flow to the T<sub>2</sub> terminal simultaneously and then the voltage and current of the both sides of the T<sub>2</sub> affects each other. The related equations are expressed in (4)-(5). The winding voltage of the T2 is exhibited in (6)

$$i_1(t) = (N_1 DV_g - V_{m2} - V_{O1})t / L_{lk1}, \quad i_{m2}(t) = V_{m2}t / L_{m2} \quad (4)$$

$$i_2(t) = (N_2 DV_g - N_3 V_{m2} - V_{O2})t / L_{lk2}, \quad i_1(t) = i_{m2}(t) - N_3 i_2(t) \quad (5)$$

$$V_{m2}(t) = \left( \left( \frac{N_1}{L_{lk1}} + \frac{N_2 N_3}{L_{lk2}} \right) DV_g - \frac{V_{O1}}{L_{lk1}} - \frac{N_3 V_{O2}}{L_{lk2}} \right) t / \left( \frac{1}{L_{m2}} + \frac{1}{L_{lk1}} + \frac{N_3^2}{L_{lk2}} \right) \quad (6)$$

#### Mode5 [t<sub>4</sub>~t<sub>5</sub>]

Mode5 starts when i<sub>1</sub> becomes zero. D<sub>2</sub> and D<sub>3</sub> are turned off softly as i<sub>1</sub> goes to zero. The peak current of the SSPR switch is the same as the reflected magnetizing current and the averaged value during one switching period becomes the slave output load current. The current equations during this mode are shown in (7)

$$i_2(t) = \frac{(N_2 DV_g - V_{O1})}{N_3^2 L_{m2}} t, \quad i_{m2}(t) = i_2(t) \quad (7)$$

#### Mode6 [t<sub>5</sub>~t<sub>6</sub>]

During Mode6, the S<sub>1</sub> voltage becomes zero and the primary side current of the transformer T<sub>1</sub> changes its direction.

#### Mode7 [t<sub>6</sub>~t<sub>7</sub>]

This mode starts when S<sub>1</sub> is turned on. Due to the positive terminal voltage of the T<sub>1</sub>, the rectifying diodes D<sub>1</sub> and D<sub>4</sub> are turned on. The current commutation seen from mode4 occurs again. The voltage and current equations are similar to (4)~(6) except the voltage of the leakage inductance in T<sub>2</sub>. The ZCS off in

the SSPR switch can be obtained by turning off S<sub>3</sub> after i<sub>2</sub> goes to zero.

## 2.2 The steady-state analysis

Utilizing the results of the modes of operation, a voltage conversion ratio is obtained. The averaged (or DC) voltage and current are required to design the proposed converter properly. Short-time and transient mode are neglected to simplify the analysis. The averaged magnetizing currents are calculated in (8)~(11) by applying the charge-balance condition in the output capacitor (C<sub>O1</sub>, C<sub>O2</sub>) and the DC blocking Capacitor (C<sub>b</sub>).

$$\langle i_{m2} \rangle (-I_{O1})(1-D_1)T_S + (-I_{O1})D_1T_S = 0, \Rightarrow \langle i_{m2} \rangle (1-D_1) = I_{O1} \quad (8)$$

$$-I_{O2}(1-D_1)T_S + \langle i_{m2} \rangle (N_3 - I_{O1})D_1T_S = 0 \quad (9)$$

$$\langle i_{m2} \rangle \cdot D_1 = N_3 I_{O2}, \quad \langle i_{m2} \rangle = I_{O1} + N_3 I_{O2} \quad (10)$$

$$\langle i_{m1} \rangle = (N_1(1-2D) + D_1(N_2/N_3 - N_1)) \cdot (I_{O1} + N_3 I_{O2}) \quad (11)$$

From (10) and (11), the two output voltage relations can be derived as in (12)

$$(I_{O1} + N_3 I_{O2}) \cdot D_1 = N_3 I_{O2}, \Rightarrow V_{O2} / V_{O1} = \frac{D_1 R_{O2}}{N_3 (1-D_1) R_{O1}} \quad (12)$$

where  $I_{O1} = V_{O1} / R_{O1}$ ,  $I_{O2} = V_{O2} / R_{O2}$

Applying the power balance condition of the input terminal and the sum of output terminals in (13), the voltage conversion ratio from the input to the master part can be derived as (14).

$$V_g \cdot \langle i_{in} \rangle = V_{O1} \cdot \langle i_1 \rangle + V_{O2} \cdot \langle i_2 \rangle \quad (13)$$

$$\frac{V_{O1}}{V_g} = \frac{2N_1 D(1-D) + DD_1(N_2 N_3 - N_1)}{(1-D_1) + \frac{D_1^2 R_{O2}}{(1-D_1) R_{O1}}} \quad (14)$$

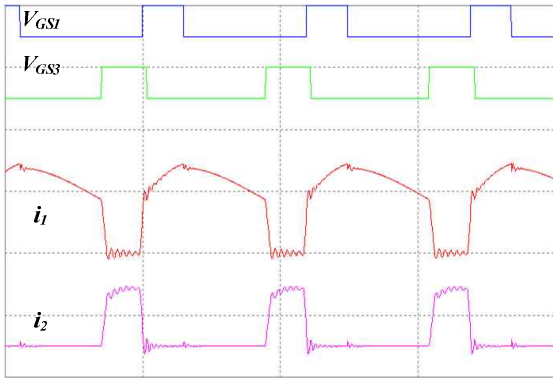
## 3. Experimental Result

The proposed converter was simulated and implemented to verify the concept and theoretical analysis. The converter is tested under 400V input voltage and switching frequency F<sub>S</sub> is 70kHz. The output voltage and currents of the converter are specified as V<sub>O1</sub>=170V, I<sub>O1</sub>=1.8A in the master output and V<sub>O2</sub>=70V, I<sub>O2</sub>=1A in the slave output. From the converter voltage gain, the normalized turns ratio are selected as N<sub>1</sub>=1, N<sub>2</sub>=1.4, N<sub>3</sub>=0.5. The other circuit parameters and hardware components are summarized in table 1.

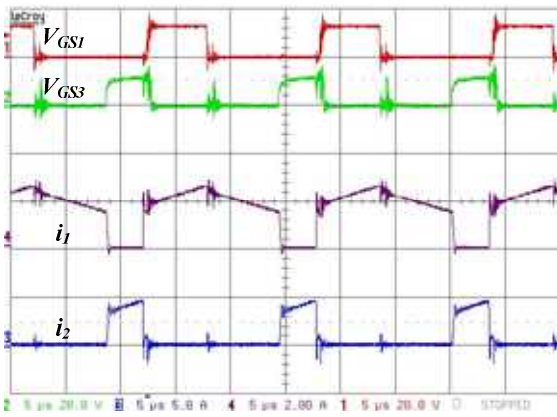
The operation of the proposed circuit through the computer simulations, as shown in Fig.3, is similar to that the experimental results. The current of the switch in the post regulator starts from zero because the current commutation in T<sub>2</sub>. When switch of the primary side is turned off, the reversed voltage in the primary side of the T<sub>2</sub> causes the current commutation. The S<sub>3</sub> should be turned off after current becomes zero for the ZCS off.

Table1. Circuit parameters

Component	Value	Component	Value
C <sub>b</sub>	100nF/15uF	L <sub>m1</sub>	406uH
C <sub>O1</sub> /C <sub>O2</sub>	2mF/1mF	L <sub>m2</sub>	340uH
S <sub>1</sub> ,S <sub>2</sub>	SWT20NM50	D <sub>1</sub> -D <sub>5</sub>	FSF10A60
S <sub>3</sub>	IRFB33N15D	Core	EER4950S/EI50



(a) Simulation result



(b) Experimental result

Fig.3 Currents of the auxiliary transformer in steady-state

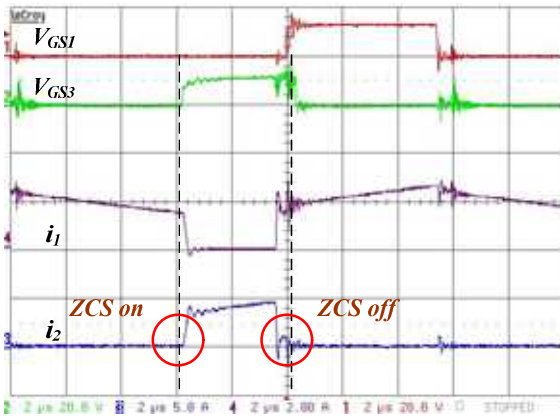


Fig.4 ZCS on and ZCS off of the SSPR switch

#### 4. Conclusion

A multiple-output converter using the SSPR with a coupled-inductor is proposed. To reduce the size and overall cost, the output filter inductor of the SSPR is integrated to the master part filter inductor. The proposed converter achieves ZCS on and off in the SSPR switch. The ZCS off in the SSPR switch eliminates the freewheeling diode in the slave part. Also the current of the rectifying diodes are turned off softly. The modes of operation of the proposed converter are analyzed to obtain the design equations. 370W prototype hardware is built to verify the analysis.

#### Reference

[1] Matuo, Hirofumi, "Comparison of Multiple-Output DC-DC Converters Using Cross Regulation", Industrial Electronics and

Control Instrumentation, IEEE Transactions on Volume IECI-27, Issue 3, Aug. 1980, pp.176 - 189

[2] D. Maksimovic, R. Erickson, "Modeling of cross-regulation in multiple-output flyback converters", APEC99, Vol 2, 14-18 March, 1999, pp.1066-1072

[3] Y. -T. Chen, D. Y. Chen, Y. -P. Wu, "Control-loop modeling of multiple-output feedback of forward converters", Power Electronics, IEEE Transaction on, Vol. 8, Issue 3, July 1993, pp. 320-328.

[4] Y. -L. Lin, K. H. Liu, "A new synchronous-switch post regulator for multi-output forward converters", APEC90, 11-16 March, 1990, pp.693-696.

[5] G. Levin, "A new secondary side post regulator (SSPR) PWM controller for multiple output power supplies", APEC95, Part 2, 5-9 March, 1995, pp.736-742.

[6] Sung-Sae Lee, Sang-Kyoo Han, Gun-Woo Moon, "A New High Efficiency Half Bridge Converter with Improved ZVS Performance", Journal of power electronics, Vol. 6, No. 3, 2006.7. pp.187-194

[7] Kim, E.-H.; Lee, J.-J.; Kwon, J.-M.; Choi, W.-Y.; Kwon, B.-H., "Asymmetrical PWM half-bridge convertor with independently regulated multiple outputs", Electric Power Applications, IEE Proceedings- Volume 153, Issue 1, 1 Jan. 2006 Page(s):14 – 22.